# New Optical Microwave Up-Conversion Solution in Radio-Over-Fiber Networks for 60-GHz Wireless Applications

Yannis Le Guennec, Ghislaine Maury, Jianping Yao, *Senior Member, IEEE*, and Béatrice Cabon, *Member, IEEE*

***Abstract*—A new method for generating optical microwave mixing based on the optical phase modulation and the fiber chromatic dispersion is further investigated. A theoretical approach based on the analysis of the optical field spectrum has lead to the evaluation of the mixing power and optimal fiber lengths of 60-GHz radio-over-fiber (RoF) networks. Results have shown adaptable fiber lengths to match the network specifications.**

***Index Terms*—Fiber chromatic dispersion, frequency modulation, optical fiber communications, optical microwave mixing, phase modulator, radio-over-fiber (RoF), 60 GHz.**

## I. Introduction

Radio-over-fiber (RoF) systems are attractive for many applications, such as broadband wireless access networks, radar, and satellite communications, and have been intensively investigated in the last few years [1], [2]. The fundamental function of an RoF network is to distribute radio signals over the optical fiber by taking advantage of its low loss wideband and immunity to electromagnetic interference caused by optics. In future RoF networks, as for millimeter-wave (mm-wave) band wireless standards of around 60 GHz, optical domain processing could also provide many functions, such as optical millimeter-wave frequency mixing in order to up or down convert subcarrier frequencies of digital signals without optical-to-electrical (O/E) and electrical-to-optical (E/O) conversions [3], [4]. The main solutions are based on the use of electrooptic modulators but suffer from the effect of fiber chromatic dispersion [5]. In this paper, we deeply investigate a novel approach for optical microwave mixing that we have already presented in [6] and [7]. This mixing system uses an electrooptic phase modulator in combination with a length of single-mode fiber (SMF) to realize the all-optical subcarrier frequency conversion. It takes advantage of the chromatic dispersion of the fiber to convert the phase-modulated signal to an intensity-modulated signal. In this paper, for the first time, we develop a theoretical analysis of the mixing process, which leads to a discussion about the possible topologies of 60-GHz RoF networks using this technique. The theoretical analysis and simulations performed aim at understanding the contributions of intensity modulation (IM), FM, and phase modulation (PM) in the frequency conversion process. Measurements are presented in order to validate this approach. The theoretical model is used to evaluate the mixing power and the optimal fiber lengths for a 60-GHz RoF network. A method based on the analysis of the optical field spectrum is also demonstrated.

Manuscript received July 18, 2005; revised November 4, 2005.

Y. Le Guennec, G. Maury and B. Cabon are with the Institute of Microelectronics Electromagnetism and Photonics, Grenoble Cedex 1, France (e-mail: yannis.leguennec@enserg.fr; maury@enserg.fr).

J. Yao is with the Microwave Photonics Research Laboratory, School of Information Technology and Engineering, University of Ottawa, Ottawa, ON K1N 6N5, Canada (e-mail: jpyao@site.uottawa.ca).

Digital Object Identifier 10.1109/JLT.2005.863301

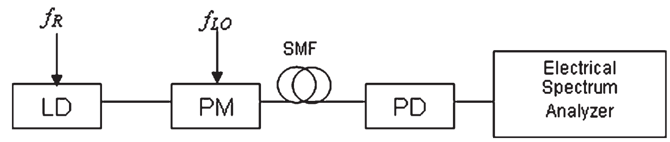


Fig. 1. Optical MW mixing system: LD, PM, SMF, and PD.

This paper is organized as follows. The experimental setup is described in Section II. The theoretical approach is presented in Section III. Simulation results and measurements are compared and discussed in order to validate this approach in Section IV, and the characteristics of the RoF network are discussed for 60-GHz wireless applications in Section V.

## II. Optical Microwave Mixing Setup Using a Phase Modulator and a Dispersive Fiber

A laser diode (LD) emitting at a wavelength of 1550 nm is directly modulated by a continuous wave (CW) microwave (MW) signal at a frequency of $f_{\mathrm{RF}}$. This direct modulation causes IM and FM known as chirp at the output of the LD. The signal from the LD is coupled into a phase modulator driven with a CW electrical signal with a frequency of $f_{\mathrm{LO}}$. The signal at the output of the phase modulator is then injected into a dispersive SMF with a dispersion coefficient of 17 $\mathrm{ps/(nm \cdot km)}$. At the output of the fiber link, the signal is detected by a 20-GHz bandwidth photodetector (PD). An electrical spectrum analyzer is then connected to the output of the PD. The schematic of the experimental setup is shown in Fig. 1.

## III. Expression of the Optical Field at the Output of the Phase Modulator

The expression of the optical field at the output of the LD is given by

$$E_{\mathrm{LD}}(t) = \sqrt{1 + m\cos(2\pi f_{\mathrm{RF}} t)}\mathrm{e}^{j\beta\sin(2\pi f_{\mathrm{RF}} t)}\mathrm{e}^{j2\pi f_0 t} \quad (1)$$

where $m$ is the IM index, $\beta$ is the FM index at $f_{\mathrm{RF}}$, and $f_0$ is the frequency of the optical carrier.

In the linear part of the LD characteristic, (1) can be approximated as follows:

$$E_{\mathrm{LD}}(t) = \left(1 + \frac{m}{2}\cos(2\pi f_{\mathrm{RF}} t)\right) \mathrm{e}^{j\beta \sin(2\pi f_{\mathrm{RF}} t)} \mathrm{e}^{j2\pi f_0 t}. \quad (2)$$

Light from the LD is coupled to the phase modulator. Then, the optical field $E_{\mathrm{PM}}(t)$ at the output of the phase modulator is given by

$$E_{\mathrm{PM}}(t) = E_{\mathrm{LD}}(t) e^{j\frac{\pi V}{V_\pi}\cos(2\pi f_{\mathrm{LO}} t)} \quad (3)$$

where $V$ is the voltage at the frequency $f_{\mathrm{LO}}$ applied to the phase modulator, and $V_\pi$ is the half-wave voltage of the modulator.

Considering (1) and (3), after a Bessel function expansion, we can write

$$\begin{aligned} E_{\mathrm{PM}}(t) = & \left(1 + \frac{m}{2}\cos(2\pi f_{\mathrm{RF}} t)\right) e^{j2\pi f_0 t} \\ & \times \left[ J_0(\beta) + 2\sum_{k=1}^{+\infty} J_{2k}(\beta)\cos(2\pi 2k f_{\mathrm{RF}} t) \right. \\ & \left. + 2j\sum_{k=0}^{+\infty} J_{2k+1}(\beta)\sin\left(2\pi(2k+1) f_{\mathrm{RF}} t\right) \right] \\ & \times \left[ J_0\left(\frac{\pi V_{\mathrm{LO}}}{V_\pi}\right) + 2\sum_{k=1}^{+\infty} (-1)^k J_{2k}\left(\frac{\pi V_{\mathrm{LO}}}{V_\pi}\right) \right. \\ & \times \cos(2\pi 2k f_{\mathrm{LO}} t) + 2j\sum_{k=0}^{+\infty} (-1)^k J_{2k+1} \\ & \left. \times \left(\frac{\pi V_{\mathrm{LO}}}{V_\pi}\right) \sin\left(2\pi(2k+1) f_{\mathrm{LO}} t\right) \right]. \end{aligned} \quad (4)$$

Useful expressions of complex envelopes of the spectral lines $\mathrm{SL}_f$ at the optical frequency $f$ can be derived from (4)

$$\begin{aligned} \mathrm{SL}_{f_0} &= J_0(\beta) J_0\left(\frac{\pi V_{\mathrm{LO}}}{V_\pi}\right) \\ \mathrm{SL}_{f_0+\varepsilon(f_{\mathrm{RF}}+f_{\mathrm{LO}})} &= \varepsilon j J_1(\beta) J_1\left(\frac{\pi V_{\mathrm{LO}}}{V_\pi}\right) \\ &\quad + j\frac{m}{4} J_0(\beta) J_1\left(\frac{\pi V_{\mathrm{LO}}}{V_\pi}\right) \\ \mathrm{SL}_{f_0+\varepsilon f_{\mathrm{RF}}} &= \varepsilon J_1(\beta) J_0\left(\frac{\pi V_{\mathrm{LO}}}{V_\pi}\right) \\ &\quad + \frac{m}{4} J_0(\beta) J_0\left(\frac{\pi V_{\mathrm{LO}}}{V_\pi}\right) \\ \mathrm{SL}_{f_0+\varepsilon f_{\mathrm{LO}}} &= j J_1\left(\frac{\pi V_{\mathrm{LO}}}{V_\pi}\right) J_0(\beta) \\ &\quad \text{with} \quad \varepsilon = \pm 1. \end{aligned} \quad (5)$$

The output power of the phase modulator at a frequency of $f_{\mathrm{LO}}$ is generated by the dominant beatings of $\mathrm{SL}_{f_0+f_{\mathrm{LO}}}$, with $\mathrm{SL}_{f_0}$ (noted $\mathrm{SL}_{f_0}\underline{\times}\mathrm{SL}_{f_0+f_{\mathrm{LO}}}$) and $\mathrm{SL}_{f_0}\underline{\times}\mathrm{SL}_{f_0-f_{\mathrm{LO}}}$. It can be seen from (5) that both beating terms have the same amplitude but are out of phase. This property causes the well-known result that there is no detected power at $f_{\mathrm{LO}}$ at the output of the phase modulator.

The output power of the phase modulator at frequency of $f_{\mathrm{RF}}$ results from the dominant beating terms $\mathrm{SL}_{f_0+f_{\mathrm{RF}}}\underline{\times}\mathrm{SL}_{f_0}$ and $\mathrm{SL}_{f_0}\underline{\times}\mathrm{SL}_{f_0-f_{\mathrm{RF}}}$. This time, both beating terms do not cancel out each other due to the presence of IM at the LD output. As a consequence, power at frequency $f_{\mathrm{RF}}$ can be detected, and this power is expressed as follows:

$$P(f_{\mathrm{RF}}) = \eta m^2 J_0^2(\beta) J_0^2\left(\frac{\pi V_{\mathrm{LO}}}{V_\pi}\right) \quad (6)$$

where $\eta$ includes the responsivity and the load impedance of the photodetector.

From (6), it can be noticed that $P(f_{\mathrm{RF}})$ is proportional to the square of the IM index of direct modulation of the LD.

The output power of the phase modulator at the mixing frequency $f_{\mathrm{RF}} + f_{\mathrm{LO}}$ results from the sum of the following dominant beating terms:

a) $\mathrm{SL}_{f_0+(f_{\mathrm{RF}}+f_{\mathrm{LO}})}\underline{\times}\mathrm{SL}_{f_0}$ and $\mathrm{SL}_{f_0} \times \mathrm{SL}_{f_0-(f_{\mathrm{RF}}+f_{\mathrm{LO}})}$, expressed as "central beating terms" because they are related to SLs, which beat with the central optical frequency;

b) $\mathrm{SL}_{f_0+f_{\mathrm{RF}}}\underline{\times}\mathrm{SL}_{f_0-f_{\mathrm{LO}}}$ and $\mathrm{SL}_{f_0+f_{\mathrm{LO}}}\underline{\times}\mathrm{SL}_{f_0-f_{\mathrm{RF}}}$ expressed as "cross beating terms," which also contribute to the mixing power.

Other beating terms which generate the mixing frequency $f_{\mathrm{RF}} + f_{\mathrm{LO}}$ are caused by higher order intermodulation products, they are very small and can be negligible.

The dominant beating terms which generate MW mixing at $f_{\mathrm{RF}} + f_{\mathrm{LO}}$ are represented in Fig. 2. The contributions in detected mixing power induced by the IM of the LD cancel in the sum of central beating terms and in the sum of cross beating terms, which is not the case for contributions induced by FM and PM. As it is illustrated in Fig. 2, the central beating terms have the same phase shift of $\Delta\varphi_1 = \Delta\varphi_2 = \pi/2$, but they are in phase opposition with cross beating terms, which have a phase shift of $\Delta\varphi_3 = \Delta\varphi_4 = -\pi/2$. As shown in (5), the amplitudes of these beating terms are equal, and the contributions in detected mixing power induced by FM and PM cancel too; consequently, there is finally no detected power at the mixing frequency $f_{\mathrm{RF}} + f_{\mathrm{LO}}$ at the output of the phase modulator.

## IV. Analysis of the Impact of the Dispersive Fiber on the Electrical Field

The dispersive fiber is used to change the phase relationship between all spectral lines $\mathrm{SL}_f$ which generate mixing power, which is fully or partially in phase. The FM of the LD and PM are then converted to IM. When the converted, signals are fed to a photodetector, and the mixing signal at $f_{\mathrm{RF}} + f_{\mathrm{LO}}$ is obtained. The transfer function of the dispersive fiber $H_{\mathrm{fib}}(f)$ [5] is given by

$$H_{\mathrm{fib}}(f) = \exp\left[j\frac{\pi D L f^2 \lambda_0^2}{c}\right] \quad (7)$$

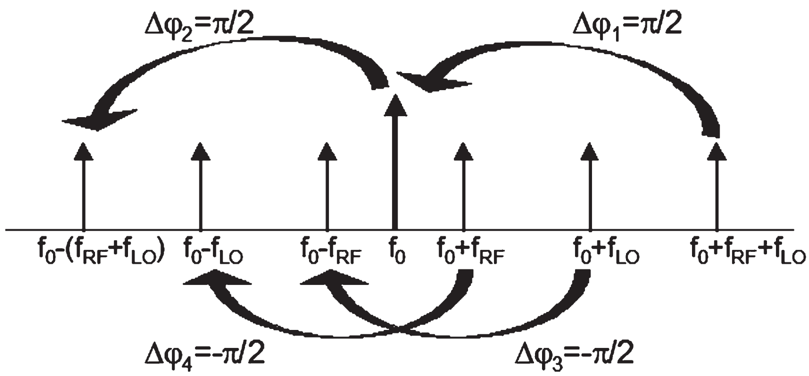


Fig. 2. Beatings of spectral lines in the optical field spectrum to generate MW mixing at $f_{\mathrm{RF}}+f_{\mathrm{LO}}$.

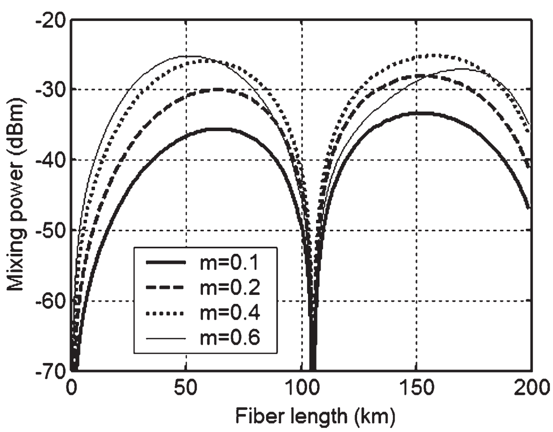


Fig. 3. FFT simulations of mixing power at 10 GHz as a function of fiber length for different IM index $m$.

where $c$ is the velocity of the light in vacuum, $D$ is the coefficient of chromatic dispersion of the fiber [$D = 17$ ps/(nm · km)], and $f$ is the modulation frequency.

After propagation over a distance $L$ in the dispersive fiber, new phase shifts are induced for all spectral lines (5). These phase shifts are calculated from the transfer function of the dispersive fiber (7), resulting in new expressions for the phase of beating terms $\Delta\varphi_1'$, $\Delta\varphi_2'$, $\Delta\varphi_3'$, $\Delta\varphi_4'$ at the output of the fiber

$$\Delta\varphi_1' = \frac{L\lambda_0^2 D\pi(f_{\mathrm{RF}}+f_{\mathrm{LO}})^2}{c} + \Delta\varphi_1 \text{ and } \Delta\varphi_2' = \pi - \Delta\varphi_1'$$
$$\Delta\varphi_3' = \frac{L\lambda_0^2 D\pi\left(f_{\mathrm{LO}}^2 - f_{\mathrm{RF}}^2\right)}{c} + \Delta\varphi_3 \text{ and } \Delta\varphi_4' = \pi - \Delta\varphi_3' \quad (8)$$

where initial phase shifts are $\Delta\varphi_1 = \Delta\varphi_2 = \pi/2$ and $\Delta\varphi_3 = \Delta\varphi_4 = -\pi/2$, as defined in Section III.

### A. Influence of the IM Index on the Mixing Power

The mixing power detected at the output of the dispersive fiber can be calculated by fast Fourier transform (FFT) simulations of the optical field at the output of the phase modulator (3), multiplied by the transfer function of the dispersive fiber (7). Fig. 3 shows the FFT simulations of the mixing power at a frequency of 10 GHz ($f_{\mathrm{RF}} = 3$ GHz and $f_{\mathrm{LO}} = 7$ GHz) for the IM index varying from 0.1 to 0.6. These simulation results have shown a shift in the amplitude of the mixing power with the IM index but no modifications in the shape of the curve as a function of fiber length for $m$ in the range (0.1–0.4). Under this condition, we can expect that the terms in (5), which contain the IM index, have a very low influence, since they would change the shape of the response of the mixing power as a function of fiber length in the FFT simulations. Fig. 4 shows the FFT simulations of the mixing power as a function of the mixing frequency for three different cases: 1) general expression of the optical field with IM, FM, and PM (1); 2) optical field with only the IM and PM contribution; and 3) optical field with only the FM and PM contribution. Simulations for 1) and 3) give identical results. As expected, with previous analysis, it can be seen that the influence of the IM term is negligible.

Therefore, the theoretical approach can be simplified by suppressing the terms containing the IM index in the expressions of the spectral lines (5).

### B. Expression of the Mixing Power

In the case of the IM modulation index lower than 0.5, as discussed before, we can use simplified expressions of spectral lines (5). As a result, the mixing power is expressed as follows:

$$P_{f_{\mathrm{RF}}+f_{\mathrm{LO}}} = A^2 \Big| \exp\left[j\Delta\varphi_1'\right] + \exp\left[j\Delta\varphi_2'\right] + \exp\left[j\Delta\varphi_3'\right] + \exp\left[j\Delta\varphi_4'\right] \Big|^2 \quad (9)$$

where $A = \eta J_0(\beta) J_0(\pi V_{\mathrm{LO}}/V_\pi) J_1(\beta) J_1(\pi V_{\mathrm{LO}}/V_\pi)$.

From the expressions of phase shifts in (7), the analytic expression of the mixing power along the dispersive fiber can be derived as follows:

$$P_{f_{\mathrm{RF}}} + f_{\mathrm{LO}} = 8A^2 \left[\sin\left(\frac{L\lambda_0^2 D\pi f_{\mathrm{RF}}(f_{\mathrm{RF}}+f_{\mathrm{LO}})}{c}\right) \times \sin\left(\frac{L\lambda_0^2 D\pi f_{\mathrm{LO}}(f_{\mathrm{RF}}+f_{\mathrm{LO}})}{c}\right)\right]^2. \quad (10)$$

Equations (9) and (10) show that the changes in the LO and RF powers only shift the amplitude of the mixing power, which is

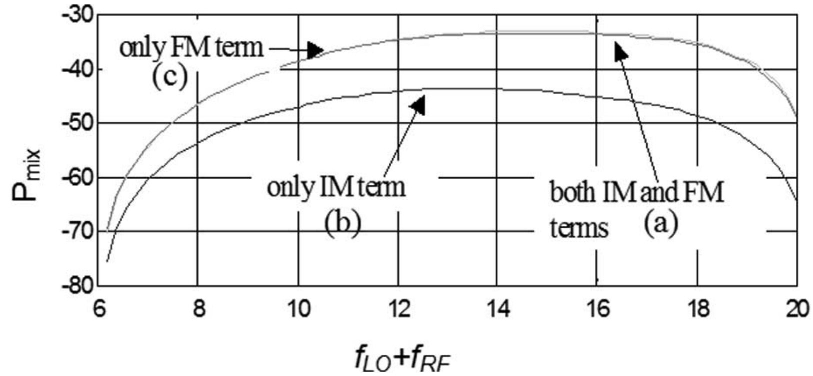


Fig. 4. Simulation of the contribution of the FM and the IM of the LD in the mixing power.

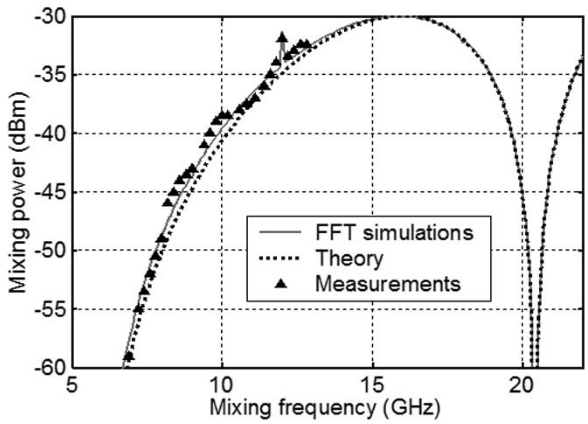


Fig. 5. Simulation/theory/measurement results of the mixing power at 10 GHz as a function of the mixing frequency.

in agreement with the FFT simulation results shown in Fig. 3 as $m$ is linked to $\beta$ through the enhancement factor of the LD [3].

Fig. 5 shows a very good agreement between the FFT simulation result and the theoretical result (10) for $f_{\rm RF}$ of 6 GHz, by changing $f_{\rm LO}$ from 300 MHz–14 GHz, with a fiber length of 25 km. On FFT simulation curve, a peak at 12 GHz is caused by the harmonic of $f_{\rm RF}$, whereas this peak is not taken into account in the theoretical analysis. The measurement results have been made by setting $f_{\rm LO}$ from 300 MHz–7 GHz, as the electrooptic phase modulator has a limited bandwidth of 7 GHz. There is a good correspondence between the measurements and the simulation/theoretical results. Therefore, the theoretical analysis has been validated with the FFT simulations and the experimental results. The analytic expression for the mixing power in (10) determines exactly the influence of the parameters, such as fiber length $L$, input frequencies, and input powers on the mixing power.

The conversion loss/gain of the system is the ratio of the mixing power photo-detected in the presence of the phase modulator and the fiber to the power measured at the output of the LD at the frequency $f_{\rm RF}$. The optimal conversion loss has been calculated to be $-20$ dB with simulations/theory. The measurements have shown a conversion loss of $-23$ dB, as the LO frequency was not set to the optimal value [6]. This conversion loss is in the same range as for usual mixing techniques [3], [4].

### *C. Fiber Lengths Causing a Mixing Power Cancellation*

From (10), we can find the expressions of fiber lengths $L_{\rm min}$ which can cause the complete cancellation of mixing power at $f_{\rm RF} + f_{\rm LO}$

$$\begin{aligned} L_{\min,k} &= \frac{kc}{f_{\rm LO}(f_{\rm RF}+f_{\rm LO})\lambda_0^2 D}\ k \in Z \quad \text{or} \\ L_{\min,m} &= \frac{nc}{f_{\rm RF}(f_{\rm RF}+f_{\rm LO})\lambda_0^2 D}\ n \in Z. \end{aligned} \tag{11}$$

The fiber lengths for mixing power cancellation are highly dependent on the input frequencies.

It is interesting to note from (11) that the first cancellation of the mixing power happens for a fiber length of $L_{\rm min,1}$ given by

$$\begin{aligned} L_{\min,1} &= \frac{c}{f_{\rm LO}(f_{\rm RF}+f_{\rm LO})\lambda_0^2 D} \quad \text{or} \\ L_{\min,1} &= \frac{c}{f_{\rm RF}(f_{\rm RF}+f_{\rm LO})\lambda_0^2 D} > L_{\rm direct} \\ &= \frac{c}{(f_{\rm RF}+f_{\rm LO})^2\lambda_0^2 D} \end{aligned} \tag{12}$$

where $L_{\rm direct}$ is the fiber length which causes the first cancellation of power in the case of a direct modulation of a LD or of an electrooptic modulator at $f_{\rm RF} + f_{\rm LO}$.

Equation (12) shows that $L_{\rm min,0}$ is longer than the fiber length $L_{\rm direct}$ which causes the first cancellation of power for a direct modulation of an LD or of an electrooptical modulator (EOM) at $f_{\rm RF} + f_{\rm LO}$ [8]. This property demonstrates a better resistance to the fiber chromatic dispersion of this new optical MW mixing technique compared to classical techniques using direct modulation or external intensity modulation.

It is important to note that the cancellation of the mixing power at $f_{\rm RF} + f_{\rm LO}$ will happen when phases of the SLs (5) will keep the values they had initially at the output of the modulator. This condition, which is found with a simple analysis of the optical field spectrum, is fulfilled when

$$\begin{aligned} \Delta\varphi_1' &= \Delta\varphi_4' + (2k+1)\pi\ k \in Z \quad \text{or} \\ \Delta\varphi_1' &= \Delta\varphi_3' + (2n+1)\pi. \end{aligned} \tag{13}$$

Considering (11), condition (13) leads directly to the expressions of $L_{\min,k}$ and $L_{\min,n}$ (12).

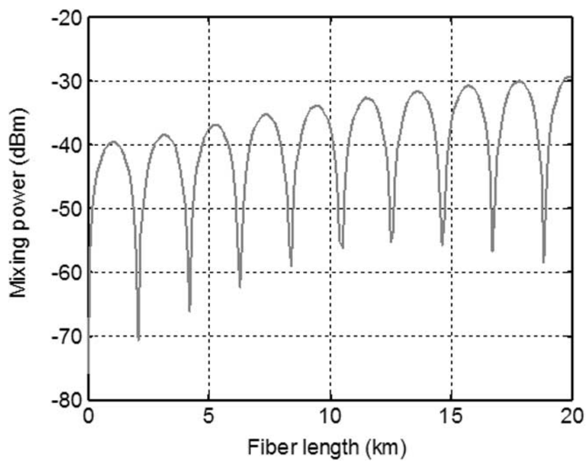


Fig. 6. FFT simulation of the mixing power at 60 GHz as a function of the fiber length.

As the fiber length for mixing power cancellation is highly dependent on the input frequencies, it can be concluded that the fiber lengths for the maxima of the mixing power and the mixing power itself also depends on the values of the input frequencies.

## V. Setup Definition of a Mixing System for Wireless 60-GHz Applications

In this section, we suppose that the desired mixing frequency at the output of the system is fixed at 60 GHz in order to demonstrate the potential of this technique in future 60-GHz RoF networks for future indoor wireless LANs [9]. We propose a method to find the optimal fiber lengths in order to build the architecture of the network. Once the optimal fiber lengths are defined, FFT simulation results give indications about the maximum conversion bandwidth and the input maximum bandwidth for the up conversion of the broadband signals.

### A. Optimal Fiber Lengths for Up-Conversion Process

The mixing power expressed in (10) is highly dependent on the choice of the fiber length, as described previously. Fig. 6 shows the simulation of the mixing power at a mixing frequency of 60 GHz as a function of the fiber length for an RF input signal at $f_{\rm RF} = 1.5$ GHz. As shown in Fig. 6, the optimal fiber lengths are found at a local maxima of the mixing power at 60 GHz. For example, for fiber length ranging from 0–20 km, ten values of the fiber lengths that cause local mixing power maxima in the range of $-40$ to $-29$ dBm are found.

These optimal fiber lengths (from 1.1 to 20 km) can be used to interconnect stations equipped with phase modulators in the RoF network and reach required conditions to generate up-converted signals which can be emitted by remote base stations in the 60-GHz bandwidth.

### B. Available Conversion Bandwidth

We suppose that the RoF link has been set with an optimal fiber length defined in Fig. 6 of 1.1, 7.4, or 17.6 km for frequency conversion at 60 GHz. It is necessary to evaluate the available conversion bandwidth, for a fixed input RF signal at 1.5 GHz, in the limit of 3-dB penalty compared to the central converted signal at 60 GHz. Fig. 7 shows the mixing power as a function of the mixing frequency for a fixed input frequency $f_{\rm RF} = 1.5$ GHz while changing the LO frequency $f_{\rm LO}$ from 53.5 to 63.5 GHz. It shows that a 3-dB conversion bandwidth around 60 GHz of 1.5 GHz for $L = 17.6$ km, of about 4 GHz for $L = 7.4$ km, and more than 7 GHz for $L = 1.1$ km, which can be suitable for future 60-GHz wireless standards where the digital signal carrier frequencies are up converted changing LO frequencies, according to the channel allocation scheme. The allocation bandwidth of 7 GHz is in the range of bandwidths proposed for future standards in the 60-GHz band.

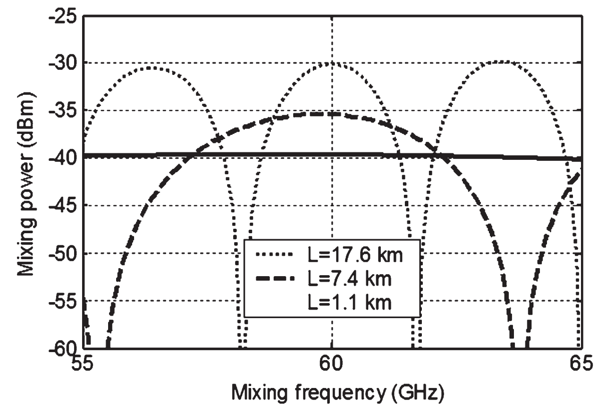


Fig. 7. FFT simulation of the mixing power as a function of the mixing frequency for three optimal fiber lengths.

## VI. Conclusion

A new technique for subcarrier frequency up conversion based on the use of a phase modulator and a dispersive fiber has been further investigated in this paper. This technique takes advantage of the chromatic dispersion properties of the fiber to convert FM and PM into IM. A theoretical approach has been developed to define the analytic expression of the mixing power at the output of the dispersive fiber; this result has been confirmed by FFT simulation results and measurements. This theoretical/simulation study has lead to optimal fiber lengths in the RoF network for the maximum mixing power. For frequency conversion from $f_{\rm RF} = 1.5$ to 60 GHz, ten values of fiber lengths ranging from 1.1 to 20 km were found, which make the architecture of the network very adaptable. The available conversion bandwidth for around 60 GHz is 1.5 GHz for a 17.6-km fiber length and more than 7 GHz for a 1.1-km fiber length.

## References

[1] L. A. Johansson and A. J. Seeds, “36-GHz 140-Mb/s radio-over-fiber transmission using an optical injection phase-lock loop source,” *IEEE Photon. Technol. Lett.*, vol. 13, no. 8, pp. 893–895, Aug. 2001.

[2] D. Wake, M. Webster, G. Wimpenny, K. Beacham, and L. Crawford, “Radio over fiber for mobile communications,” in *Proc. IEEE Int. Topical Meeting Microwave Photonics*, Ogunquit, ME, Oct. 2004, pp. 157–160.

[3] G. Maury, A. Hilt, T. Berceli, B. Cabon, and A. Vilcot, “Microwave-frequency conversion methods by optical interferometer and photodiode,” *IEEE Trans. Microw. Theory Tech.*, vol. 45, no. 8, pp. 1481–1485, Aug. 1997.

[4] G. K. Gopalakrishnam, W. K. Burns, and C. H. Bulmer, "Microwave-optical mixing in $LiNbO_3$ modulators," *IEEE Trans. Microw. Theory Tech.*, vol. 41, no. 12, pp. 2383–2391, Dec. 1993.
[5] Y. Le Guennec, G. Maury, and B. Cabon, "Improvement of dispersion resistance in analog radio-over-fiber upconversion links," *J. Lightw. Technol.*, vol. 21, no. 10, pp. 2211–2216, Oct. 2003.
[6] Y. Le Guennec, J. Yao, H. Nasrallah, G. Maury, and B. Cabon, "Optical upconversion of a BPSK modulated sub-carrier employing a phase modulator and a dispersive fiber," in *Proc. IEEE Int. Topical Meeting Microwave Photonics*, Seoul, Korea, Oct. 2005. to be published.
[7] J. P. Yao, G. Maury, Y. Le Guennec, and B. Cabon, "All-optical subcarrier frequency conversion using an electrooptic phase modulator," *IEEE Photon. Technol. Lett.*, vol. 17, no. 11, pp. 2427–2429, Nov. 2005.
[8] J. L. Corral, J. Marti, and J. M. Fuster, "General expressions for IM/DD dispersive analog optical links with external modulation or optical upconversion in a Mach Zehnder electrooptical modulator," *IEEE Trans. Microw. Theory Tech.*, vol. 49, no. 10, pp. 1968–1976, Oct. 2001.
[9] A. Kim, Y.-H. Joo, and Y. Kim, "60-GHz wireless communication systems with radio-over-fiber links for indoor wireless LANs," *IEEE Trans. Consum. Electron.*, vol. 50, no. 2, pp. 517–520, May 2004.

**Yannis Le Guennec** was born in Le Havre, France, on May 20, 1977. He received the engineering degree from the Grenoble National School for Physics, Grenoble, France, in 2000 and the Ph.D degree in optics, optoelectronics, and microwaves from the Institute for Microelectronics, Electromagnetism, and Photonics (IMEP), the Institut National Polytechnique de Grenoble (INPG), Grenoble, France in 2003.

In 2004, he held a postdoctoral position with the National University of Ireland, Maynnoth. He is currently Assistant Professor at the IMEP, where his fields of interest are microwave photonics, all-optical signal processing, ultra wide band (UWB) communications, and UWB over fiber.

**Ghislaine Maury** received the degree in telecommunications engineering from Ecole Nationale Superieure des Télécommunications, Paris, France, and the Ph.D. degree in electronics from the Institut National Polytechnique de Grenoble (INPG), International Institute University, Paris, in 1998.

She is presently an Assistant Professor at the Institute of Microelectronics, Electromagnetism, and Photonics (IMEP) Laboratory, Grenoble, France. Her research interests include microwave photonics and digital signals.

**Jianping Yao** (M'99–SM'01) received the Ph.D. degree in electrical engineering from the Université de Toulon, Toulon, France, in 1997.

He is an Associate Professor in the School of Information Technology and Engineering, University of Ottawa, Ottawa, ON, Canada. From January 1998 to July 1999, he was a Research Fellow and from July 1999 to December 2001, he was an Assistant Professor, both with the School of Electrical and Electronic Engineering, Nanyang Technological University, Singapore. He was an Invited Professor in the Institut National Polytechnique de Grenoble, Grenoble, France, from January to March 2005. He is the author or coauthor of over 100 papers in refereed journals and conference proceedings. His current research interests include optical signal processing, optically controlled phased array antennas, photonic generation of microwave signals, radio-over-fiber (RoF) systems, fiber lasers and amplifiers, and fiber-optic sensors.

Dr. Yao is a member of the International Society for Optical Engineering (SPIE) and the Optical Society of America (OSA).

**Béatrice Cabon** (S'93–M'95) received the Ph.D. degree in microelectronics from the Institut National Polytechnique de Grenoble (INPG), Grenoble, France, in 1986.

From 1986 to 1989, she held a post-doctoral position with the National Center of Telecommunications, Grenoble. In 1989, she joined the INPG, Grenoble, where she is currently a Professor. She is Head of a research group on RF, microwaves, and microwave-photonics techniques at the Institute for Microelectronics, Electromagnetism, and Photonics (IMEP) Laboratory. She has been Coordinator of the club "optics and microwaves" of the French Optical Society (S.F.O) since 1999. She has been Coordinator of the IST-2001-32786 "Network of Excellence on broadband Fiber Radio Techniques and its Integration Technology" (NEFERTITI) with 28 organizations in over nine countries, funded by the European Commission (from 2002 to 2005). Currently, she is Coordinator of the network of excellence FF6-IST-26592 InfraStructures for broadband access in wireless/photonics and Integration of Strengths in Europe (ISIS) (2006–2009) with 19 organizations in 12 countries and funded by the European Commission. Her research interests include microwave photonics, photonic-microwave signal processing, and optical links for high bit rate signals. She has contributed to over 200 technical publications and is the Editor of four books in these areas.

Prof. Cabon is a member of the IEEE Lasers and Electro-Optics Society (IEEE LEOS) and the IEEE Microwave Theory and Techniques Society (IEEE MMT-S). She is a member of the Technical Committee on Microwave Photonics of the IEEE Microwave Theory and Techniques Society (IEEE MMT-S): IEEE MTT-3. She is member of the Technical Program Committee (TPC) of the IEEE International Topical Meeting on Microwave Photonics. She organizes this conference in 2006 as well as the International Microcoll Conference.